Vol. 25: 229–243, 2004 | CLIMATE RESEARCH Clim Res | Published January 23

Variability of extreme precipitation events in Tijuana, Mexico

Tereza Cavazos*, David Rivas

Departmento de Ocenografía Física, CICESE, km 107 Carretera Tijuana-Ensenada, Ensenada, BC, 22860, Mexico

ABSTRACT: We investigated the variability of 1 d precipitation extremes (top 10%) in Tijuana (Mexico) during 1950–2000. Interannual rainfall variability is associated with El Niño/Southern Oscillation (ENSO), which explains 30% of rainfall and 36% of 1 d extreme precipitation variance. Interannual precipitation exhibits a large change, with a relatively dry period and less variability during 1950–1976, followed by a relatively wet period and more variability during 1976–2000. All extremely wet years (>1 SD) and the largest frequency of 1 d extremes occurred after 1976–1977, with 6 out of 8 extremely wet years characterized by El Niño episodes and 2 by neutral conditions. However, more than half of the 1 d extremes during 1950–2000 occurred in non-ENSO years, providing evidence for the fact that neutral conditions contribute significantly to extreme climatic variability in the region. Extreme events that occur in neutral (strong El Niño) conditions are associated with a 'pineapple express' and a 'neutral Pacific/North America (PNA)' (negative tropical/northern hemisphere [TNH]) teleconnection pattern that links an anomalous tropical convective forcing west (east) of the date line with a strong subtropical jet over the study area. The neutral PNA is a variant of the typical ±PNA teleconnection pattern; it is shifted northwestward of the +PNA (typical of El Niño) and southeastward of the –PNA (typical of La Niña) and is characterized by a strong ridge over the Gulf of Alaska and a deep low over California. We believe that the trough in the jet, typical of extreme events during neutral and strong El Niño years, is further intensified by thermal interaction with regional anomalies of a warm California Current off Baja California, low-level moisture advection from the subtropical warm sea-surface region, and intense convective activity over the study area.

KEY WORDS: Climatic variability · Extreme precipitation · ENSO · Non-ENSO · Tijuana · Mexico

1. INTRODUCTION

Extreme climate events around the world have received great public attention in the last decade due to rising economic losses, coupled with an increase in deaths as a result of these events (Karl & Easterling 1999). As population and urban centers continue to grow in areas where landscape use and societal infrastructure have considerably changed, the potential for catastrophic impacts during extreme conditions has also increased (Easterling et al. 2000). This is the case in Tijuana, a border city (with San Diego, California) with the most dynamic economy and largest population growth in Mexico, mainly due to immigration fueled by the growing *maquiladora* industry (Saldaña 1998). Moreover, Tijuana's topography, characterized by steep slopes and canyons with few measures to control erosion, promotes runoff and floods during extreme conditions. The worst flooding in Tijuana in the last 50 yr occurred in January 1993 during a moderate El Niño episode. The event produced 87 mm of rain in 2 d, more than one-third of the annual rainfall, and 210 mm in half a month. Life in the city was practically paralyzed for almost 1 mo (Bocco et al. 1993). During El Niño events, the Pacific storm track extends much farther downstream than during 'normal' winters; this has brought more active landfalling cyclones to California (and NW Baja California), resulting in flooding, landslides, and beach erosion (e.g. Chang et al. 2002, Lizárraga Arciniega et al. 2003).

*Email: tcavazos@cicese.mx

The most studied precipitation-related climatic impacts in the area are those associated with El Niño/Southern Oscillation (ENSO); this is because the interannual scale (2–7 yr) contributes more than 40% of the rainfall variability, and ENSO explains about 30% of that variance (e.g. Cayan et al. 1998). Annual rainfall in southern California and NW Baja California is commonly above (below) normal during El Niño (La Niña) events with some exceptions (e.g. Schonher & Nicholson 1989, Gershunov & Barnett 1998, Pavía & Badan 1998, Minnich et al. 2000, Pavía 2000). During strong El Niño episodes, heavy precipitation is also common in southern California (e.g. Cayan et al. 1999, Higgins et al. 2000, Gershunov & Cayan 2003), as well as in NW Baja California (e.g. Pavía & Badan 1998) and Tijuana (e.g. Bocco et al. 1993). Gershunov & Cayan (2003) document that the frequency of heavy daily precipitation in southern California and the SW US responds to ENSO as well as to non-ENSO interannual and interdecadal variability in the North Pacific. Higgins et al. (2000) emphasize that extreme precipitation events in southern California occur at all phases of the ENSO cycle, but most of these events occur during neutral winters prior to the onset of El Niño, and are linked to intraseasonal (i.e. Madden–Julian Oscillation, MJO) and interannual (ENSO) fluctuations (Mo & Higgins 1998).

The purpose of this study is to investigate the interannual variability of extreme precipitation (above the 90th percentile: P90) and to diagnose the regional and large-scale climate anomalies associated with 1 d heavy precipitation events in Tijuana, Baja California, Mexico. This work is different from previous studies in that we focus on the interannual change of 1 d precipitation extremes in a large urban center that is prone to runoff and floods. We use annual precipitation and unfiltered 1 d events to obtain the frequency of precipitation extremes (P90) in Tijuana and their relationship with ENSO and non-ENSO (neutral) conditions over the last 50 yr, and to determine whether there has been an increase in the frequency of extreme events as suggested by the storm-track results of Graham & Diaz (2001), and by the late-1970s heavy precipitation 'shift' in California reported by Gershunov & Cayan (2003). We also diagnose the possible ocean–atmosphere forcings associated with 1 d extreme rainfall events through daily large-scale mean composite and evolution anomalies of several fields during strong El Niño and neutral years. The meteorological station used in this analysis is located at the city limits, thereby circumventing the possibility of urban-induced increases in precipitation (e.g. Karl et al. 1995). This work is organized as follows: Section 2 describes the data used and the definition of extreme events; Section 3 describes the interannual rainfall variability; Section 4 discusses the variability and impact of 1 d extreme events in Tijuana and their modulation by the ENSO cycle; Section 5 explains the teleconnections and possible forcing mechanisms associated with 1 d extreme events; and Section 6 states the conclusions of this study.

2. DATA

Daily and monthly precipitation values used in this work are from the meteorological station at Presa Rodríguez (Rodríguez Dam) near the city of Tijuana, Baja California. This station has gathered data since 1929, but our analysis is based on the 1950–2000 information, as there are fewer gaps for this period. Data were provided by the Servicio Meteorológico Nacional (Mexico). Data quality control consisted of comparing the time series with monthly data from Chula Vista, California, which is located 15 km north of Tijuana. The Chula Vista data for the 1948–2000 period were obtained from the Western Regional Climate Center (WRCC) in San Diego, California. Since rainfall occurs mostly during winter (November–April), the annual precipitation is constructed from July to the following June, as suggested by Pavía & Badan (1998). The correlations of the monthly and annual precipitation in Chula Vista and Tijuana were 0.88 and 0.93, respectively. Mean winter precipitation was the same at both stations (220 mm), but the SD of the annual and winter precipitation was 9 mm larger for Tijuana than for Chula Vista, possibly because the Rodríguez Dam station is farther inland from the coast (about 20 km) than Chula Vista (10 km). Since the monthly and annual time series for both locations are highly correlated, we used the Chula Vista data to fill in almost 5 yr of gaps for Tijuana (1956, 1972–1975), but we did not include this information in the calculation and diagnosis of 1 d extreme precipitation events.

The ENSO phase is represented by the Southern Oscillation Index (SOI), defined as the standardized difference in sea-level pressure anomalies between Tahiti and Darwin, Australia. Sustained negative (positive) values of the SOI indicate El Niño (La Niña) episodes. Monthly series of the SOI were obtained from the Climate Prediction Center's website (http://www.cpc.noaa.gov/data/indices). Daily large-scale composite maps of mean and anomaly atmospheric and oceanic conditions during extreme events were obtained directly from the website of the NOAA-CIRES Climate Diagnostics Center in Boulder, Colorado (http://www.cdc.noaa.gov/Composites/Day), which uses reanalyzed daily data from the National Centers for Environmental Prediction (NCEP/NCAR). Outgoing longwave radiation (OLR) has been frequently used as a proxy for large-scale tropical convective activity. Interpolated OLR (Liebmann & Smith

1996) for the 1974–2000 period was also obtained from the NOAA-CIRES website. Both the NCEP/NCAR reanalyzed data and the interpolated OLR have a 2.5° latitude × 2.5° longitude resolution.

We define annual and winter precipitation extremes as those above or below 1 SD, representing approximately the top 10% (wet) and bottom 10% (dry) of the data records for Tijuana. Higgins (2001) considers that when SOI ≤ –0.5, there is an El Niño event, and when SOI ≥ 0.5, there is a La Niña event. We retain thresholds for strong El Niño events when SOI ≤ –1 and strong La Niña when SOI ≥ 1; values between –1 and –0.5 are considered to represent a moderate El Niño, and values between –0.5 and 0.5 are considered as neutral or non-ENSO years. One-day rainfall extremes are defined as those above the 90th percentile (P90) of the population of days with daily precipitation >0. The return period of an extreme daily event is defined as the average time in which the magnitude of a given event could be equaled or exceeded at least once. If an event $\geq x$ occurs once in T_r yr, its probability of occurrence is $P(x \geq X) = 1/T_r$. The data distribution is described by means of a Weibull distribution function, also known as empirical distribution function, which is very efficient for non-specified functions (Aparicio-Mijares 1997). The return period of an extreme event is given by $T_r = (n + 1)/i$, where n is the total number of events and i is the ranked number of the record in ascending order.

3. INTERANNUAL RAINFALL VARIABILITY

Tijuana is characterized by a semiarid Mediterranean climate and has an annual precipitation of 231 ± 115 mm (Fig. 1). The expansion of the polar vortex and the southward migration of the North Pacific high-pressure belt during winter allow the penetration of westerly humid air and mid-latitude storm tracks in the region; 90% of the annual precipitation falls during winter. From 1950 until the mid-1970s, Tijuana experienced a relatively dry period (Fig. 1), as did NW Baja California (Reyes & Troncoso 2003) and most of northern Mexico and the SW US (e.g. Swetnam & Betancourt 1998). According to the National Water Commission (CNA), Rodríguez Dam, where Tijuana's precipitation data come from, was at its lowest capacity in the early 1960s; therefore, the local government of Baja California built a well in La Misión (south of Tijuana), and in 1975 the Mexican Federal Government began the construction of the Colorado River–Tijuana Aqueduct to supply water to the city.

Mean precipitation and its variability increased after 1976 (Fig. 1), with a strong impact on the frequency of extreme events, as will be seen later. From 1976 to 1980,

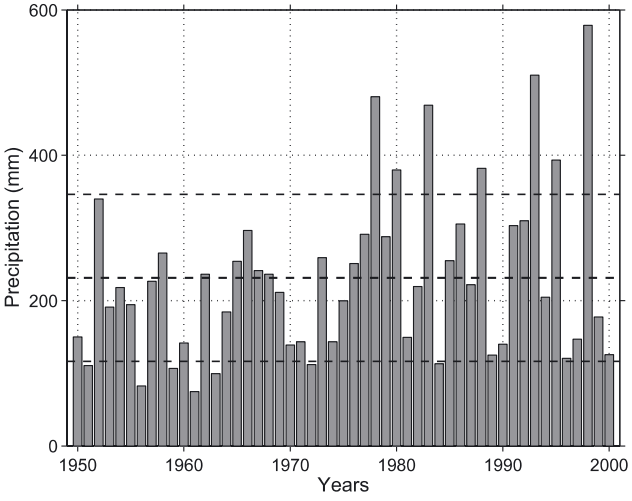

Fig. 1. Annual precipitation (July–June) in Tijuana, Mexico. Broken lines: mean ± SD = 231 ± 115 mm; 2000 corresponds to July–June 1999–2000

precipitation was above normal, and by 1980, the Rodríguez Dam was at full capacity; the floodgates of the dam were opened and downstream flooding destroyed several homes (Dedina 1995). After 1980, 2 strong El Niño episodes (1983 and 1998) and a moderate El Niño (1993) were responsible for the wettest years of the period, with annual rainfall >2 SD above the long-term mean. A spectral analysis of winter rainfall (Fig. 2), based on the Blackman–Tukey method (Chatfield 1975), shows that 52% of the variance above the white noise spectral line is linked to the interannual scale (2–7 yr); as already mentioned, ENSO explains about 30% of the rainfall variability in the region (e.g. Schonher & Nicholson 1989, Cayan et al. 1998, Gershunov & Barnett 1998, Pavía & Badan 1998, Minnich et al. 2000, Pavía 2000); thus, 22% of the interannual variance is associated with non-ENSO influences. On the other hand, 23% of the variability comes from decadal fluctuations, consistent with the results of Reyes & Troncoso (2003) for other parts of NW Baja California and of Cayan et al. (1998) for southern California. Decadal changes, similar to the ones noted from Fig. 1, have been associated with ENSO-like ocean–atmosphere decadal fluctuations in the North Pacific basin (e.g. Zhang et al. 1997, Cayan et al. 1998, Dettinger et al. 1998, Gershunov & Barnett 1998, Reyes & Troncoso 2003).

4. VARIABILITY OF ONE-DAY PRECIPITATION EXTREMES AND IMPACTS

The threshold for 1 d extremes (P90) for 1950–2000 was 10 mm. The annual cycle of daily extremes (Fig. 3) exhibited a seasonal distribution similar to the annual

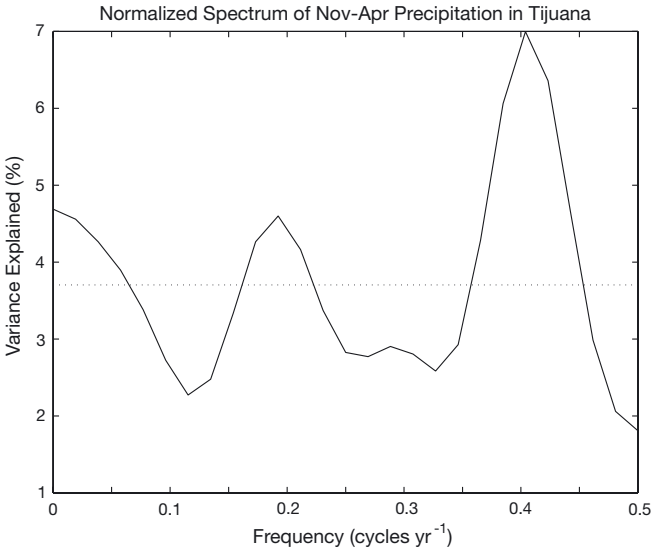

Fig. 2. Spectral analysis of winter precipitation (November–April) for 1950–2000. Dotted line: white-noise spectrum equivalent to the total variance

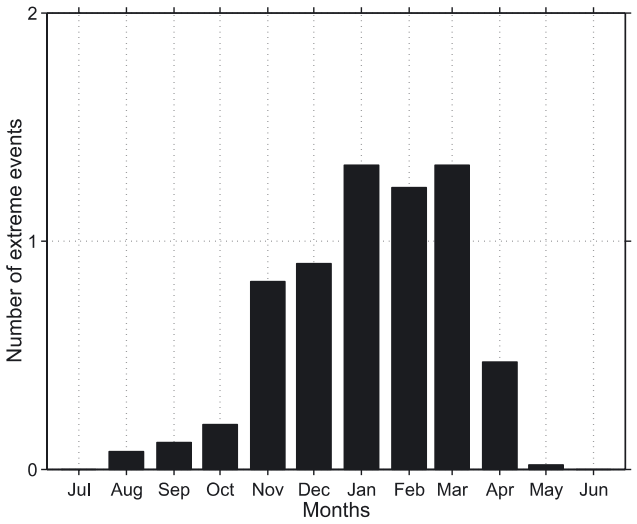

Fig. 3. Annual cycle (July–June) of the frequency of 1 d extreme precipitation events (P90) for 1950–2000

cycle of rainfall (not shown), with maxima in January–March. At least 1 extreme rainy event is expected each year in Tijuana during these months. In the 50 yr period there was a significant (100%) increase in the total frequency of extremes during 1976–2000 (Fig. 4a, Table 1). These results are consistent with Chang & Fu (2003), who documented a significant increase in the storm-track activity in the North Pacific over the 1979–1999 period. In particular, Chang et al. (2002) and Chang & Fu (2003) indicated that in the last 50 yr, storm-track activity was strongest in the 1990s and weakest in the 1960s. The difference shows an intensified winter storm-track activity in California and NW Baja California in the 1990s. Moreover, Graham & Diaz (2001) showed an increasing trend of North Pacific winter cyclones since 1948, and Gershunov & Cayan (2003) also supported the existence of a positive trend in the frequency of heavy wintertime precipitation events in California.

As with the annual rainfall (Fig. 1), the most extreme years in the 50 yr period corresponded to 2 strong El Niños and 3 moderate El Niños (Fig. 4b). The largest frequency of 1 d extreme events was observed in 1998. In February 1998, heavy rainstorms with strong winds caused flash flooding in Tijuana, killing at least 13 people and forcing 5000 to 8000 people from their homes; flooding conditions were exacerbated by insufficient

Table 1. Total frequency composites of 1 d extreme events (P90 > 10 mm d^{-1}) in Tijuana during strong El Niño, moderate El Niño, and neutral years, based on the mean November–April SOI. Relative frequency = frequency/*n* yr of the composite. Last 3 columns show the mean daily precipitation of the composite events, the mean duration based on consecutive rainy days after onset of each extreme event, and the years of occurrence. Data for 1956 and 1971–1975 were not available

Type of year (*n*)	Frequency	Relative frequency	Mean precipitation (mm d^{-1})	Mean duration (d)	Years
1950–1971					
Strong El Niño (1)	9	9.0	20.0	7.6	Jul–Jun 1966
Moderate El Niño (3)	24	8.0	7.5	2.6	1952, 1958, 1970
Neutral (10)	57	5.7	18.0	7.0	1953, 1954, 1957, 1959, 1960, 1962, 1963, 1964, 1965, 1967
1976–2000					
Strong El Niño (4)	52	13.0	22.0	4.5	1983, 1987, 1992, 1998
Moderate El Niño (5)	58	11.6	19.0	3.5	1978, 1988, 1993, 1994, 1995
Neutral (11)	77	7.0	21.4	4.2	1977, 1979, 1980, 1981, 1982, 1984, 1986, 1990, 1991, 1996, 1997

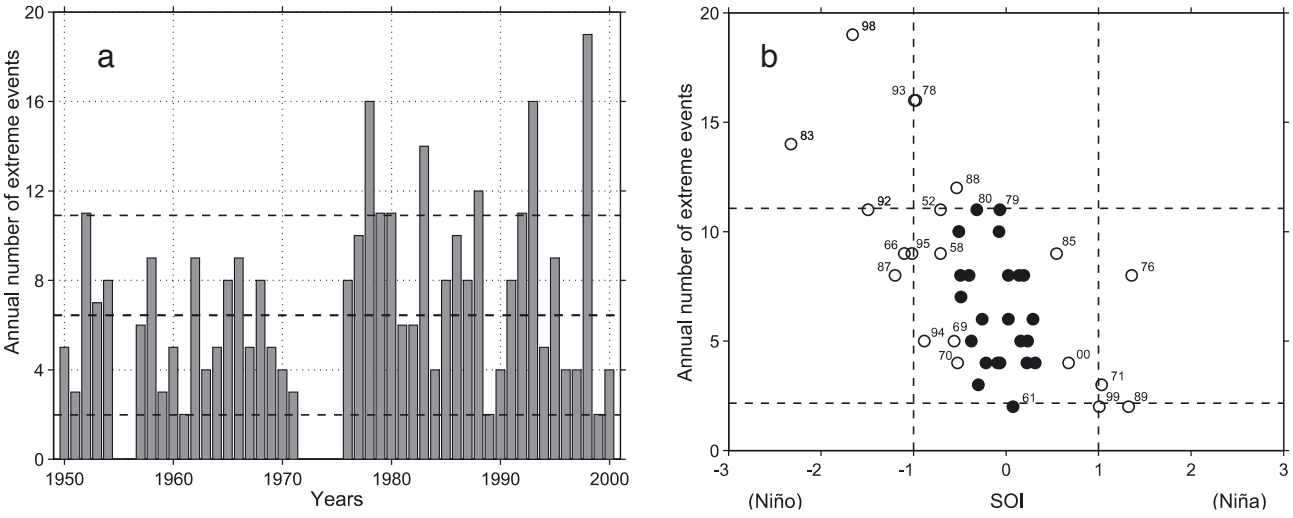

Fig. 4. (a) Annual number of 1 d extreme precipitation events (P90 > 10 mm d^{-1}). Broken lines: mean ± SD; gaps indicate lack of data. (b) Number of extreme events (1952–2000) as a function of the mean winter (November–April) SOI. Broken lines: ± SD; ●: neutral years

storm drains and buildings on hillsides (AP Worldstream 1998). Intense beach erosion was also reported in Tijuana and Rosarito (Lizárraga Arciniega et al. 2003). Flash flooding in Tijuana has become a serious hazard, especially for low-income families, who tend to occupy marginal pieces of land in steep terrains. Tijuana's Civil Protection Office identified a number of hazard zones after the torrential rains of El Niño 1993 (Fig. 4); some of these risk areas were affected again by the winter storms of El Niño 1998 (Institute for Regional Studies of the Californias, http://www-rohan.sdsu.edu/index.html).

The correlation between annual frequency of 1 d extreme events and SOI was –0.60 and statistically significant ($p < 0.05$). Although in the last 50 yr the largest number of heavy rainfall events occurred during strong and moderate El Niño winters, extremes were also common during neutral years as indicated by the solid circles in Fig. 4b. This is further illustrated in Table 1, which shows that the most important contribution to daily extremes during 1950–1971 was from 10 neutral years with a mean duration of 7 d $event^{-1}$ and a mean precipitation of 18 mm d^{-1}. In contrast, during 1976–2000 the largest contribution to extreme events (58%) was from 4 strong and 5 moderate El Niño events; a 42% contribution was from neutral years, totalling 11 yr. The relative frequency in Table 1 also indicates that on an annual basis El Niño years tend to exert a stronger impact on the number of extreme events than neutral years. On average, the mean duration of these 2 types of extreme events was 4.3 d, with a mean precipitation of 21 mm d^{-1}. The mean duration of extreme events during neutral and strong El Niño conditions decreased in the second period, but the intensity increased, possibly having an impact on surface runoff and erosion of topsoil. The return probability curve (Fig. 5) indicates that 1 d extremes characterized by less than 45 mm may return at interannual timescales. Daily extremes with more than 60 mm depart from the theoretical logarithm curve; one of these rare events occurred in a strong El Niño (03/83), 2 during moderate El Niño (01/93, 02/95), and 3 during neutral (02/91, 01/80, 01/67) years. The CNA (1995) documented that the severe floods of 01/80, 03/83 and 01/93 produced devastating effects

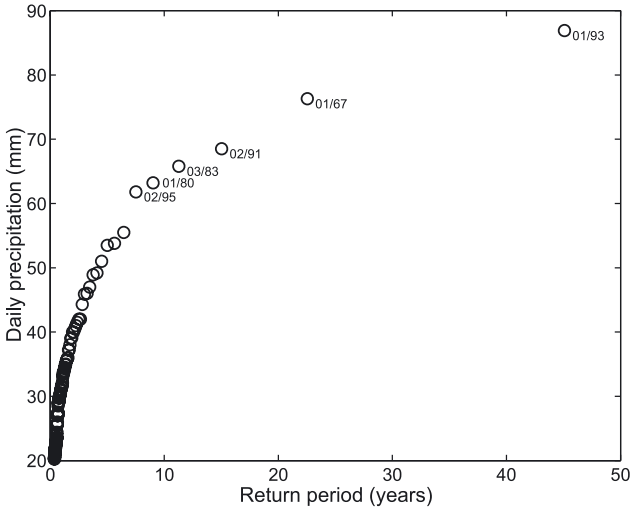

Fig. 5. Return period of 1 d precipitation extremes (P95 > 20 mm d^{-1}) for 1950–2000. The most extreme events are identified by the month and year of occurrence

on natural habitat, structures, personal property, and transportation facilities in the Tijuana River Valley (located at the western end of the US–Mexican border). Three of the 6 heaviest rainfall events and almost half of the total frequency of extremes during 1950–2000 occurred in neutral years, evidencing the importance of the contribution of neutral conditions to extreme climatic variability in the region. Unfortunately, awareness during neutral conditions has been overlooked because much of the media's attention has focused on the impacts of strong El Niños, but also because of the large variability of extreme events during neutral conditions (Fig. 4). This is supported by Gershunov & Cayan's (2003) results, which indicate that the prediction skill of heavy precipitation in southern California and the SW US is significantly better during extremes of ENSO than during normal years. The same authors state that predictability during neutral years appears to be associated with North Pacific SST (sea surface temperature) interannual and decadal variability uncorrelated with ENSO.

5. TELECONNECTIONS ASSOCIATED WITH ONE-DAY EXTREMES

5.1. Synoptic characteristics

At synoptic timescales, extreme wet events in the study area are associated with a western trough near the coast of California and Baja California (Fig. 6) and, on many occasions, with a cut-off low in the Pacific Northwest (Fig. 6a) and a ridge (or blocking high) in the eastern North Pacific (Fig. 6b,d). One-day extremes are also characterized by a surface cyclone near the coast of California, indicating a southward-displaced North Pacific high (not shown). Anomalies in the Pacific, especially near the continent due to the thermal contrast and exit region of the jet stream, generate eddies, ridges and troughs. The midtropospheric trough and surface cyclone typical of extreme events during strong El Niños between 1976 and 2000 are linked to a warm California Current, a cold North Pacific Ocean, and an anomalous equatorial heating (Fig. 7a). In contrast, the main SST feature linked to extreme events of neutral years is a warm California Current off the west coast of Baja California (Fig. 7b). Temperature gradients provide a thermal forcing for cyclones and transient eddies, which may produce large meridional transport of momentum, heat, and moisture.

On interannual timescales, the Pacific jet stream and the associated storm track shift equatorward and farther downstream during El Niño years (e.g. Trenberth & Hurrell 1994, Zhang & Held 1999), apparently in response to local enhancement of the Hadley circulation (e.g. Bjerknes 1969). This brings more active landfalling winter cyclones to California (Chang et al. 2002). Graham & Diaz (2001) reported intensified upper-tropospheric zonal winds (ZW200) in the North Pacific between 25 and 40° N during 1980–1998, consistent with the increased storm track activity documented by Chang & Fu (2003). Similarly, our results also show an increased number of extreme events in the same period (Table 1) characterized by enhanced ZW200 anomalies (Fig. 8), which indicate a strong subtropical jet during extreme events of strong El Niño and neutral years. In both types of extreme events the core of the jet has maximum wind anomalies of 12 m s^{-1} near Baja California. In neutral conditions, the Pacific jet is located downstream much farther NE of the continental divide, as is common in neutral years.

Composite OLR anomalies (Fig. 9) show that a major difference between extreme events is that equatorial convective activity during extremes of strong El Niños is very intense and centered at 160° W (Fig. 9a), while during neutral years the convective forcing is weaker and located between 140 and 150° E (Fig. 9b). This is consistent with the results of Mo & Higgins (1998) and Higgins et al. (2000) for extreme events in southern California. They associated the tropical forcing west of the Dateline to intraseasonal oscillations (IO) due to the MJO. The MJO is a westerly wave in the atmosphere with a 30 to 60 d period associated with enhanced convection originating over the Indian Ocean (Madden & Julian 1972); it tends to be more active during neutral years (Kousky & Kayano 1994), especially just prior to El Niño (Higgins et al. 2000).

Tropical teleconnections to the study area are possible through wave trains (e.g. Trenberth & Hurrell 1994) that extend from the tropical forcing to the PNA region, as suggested by the 200 hPa streamfunction (STR200) anomalies in Fig. 10. Teleconnections are important because they modulate the stationary atmospheric circulation in the midlatitudes producing climate anomalies in faraway regions. Positive SST anomalies characteristic of extreme events during strong El Niño are associated with an enhanced local Hadley cell that generates an upper-level anticyclone (Fig. 10a) near the zone of maximum heating and convective activity in the equatorial region (Fig. 9a). The anomalous upper-level outflow in the northern branch of the Hadley cell interacts with the background flow of the midlatitudes, resulting in strong subtropical convergence and, possibly, in a redistribution of the preferred long waves in the upper-level westerlies. The strong upper tropospheric divergence in the tropics and convergence in the subtropics act as a Rossby wave source (Trenberth et al. 1998) producing a wave train of alternating high and low streamfunction (STR200; Fig. 10a) and geopotential anomalies. The

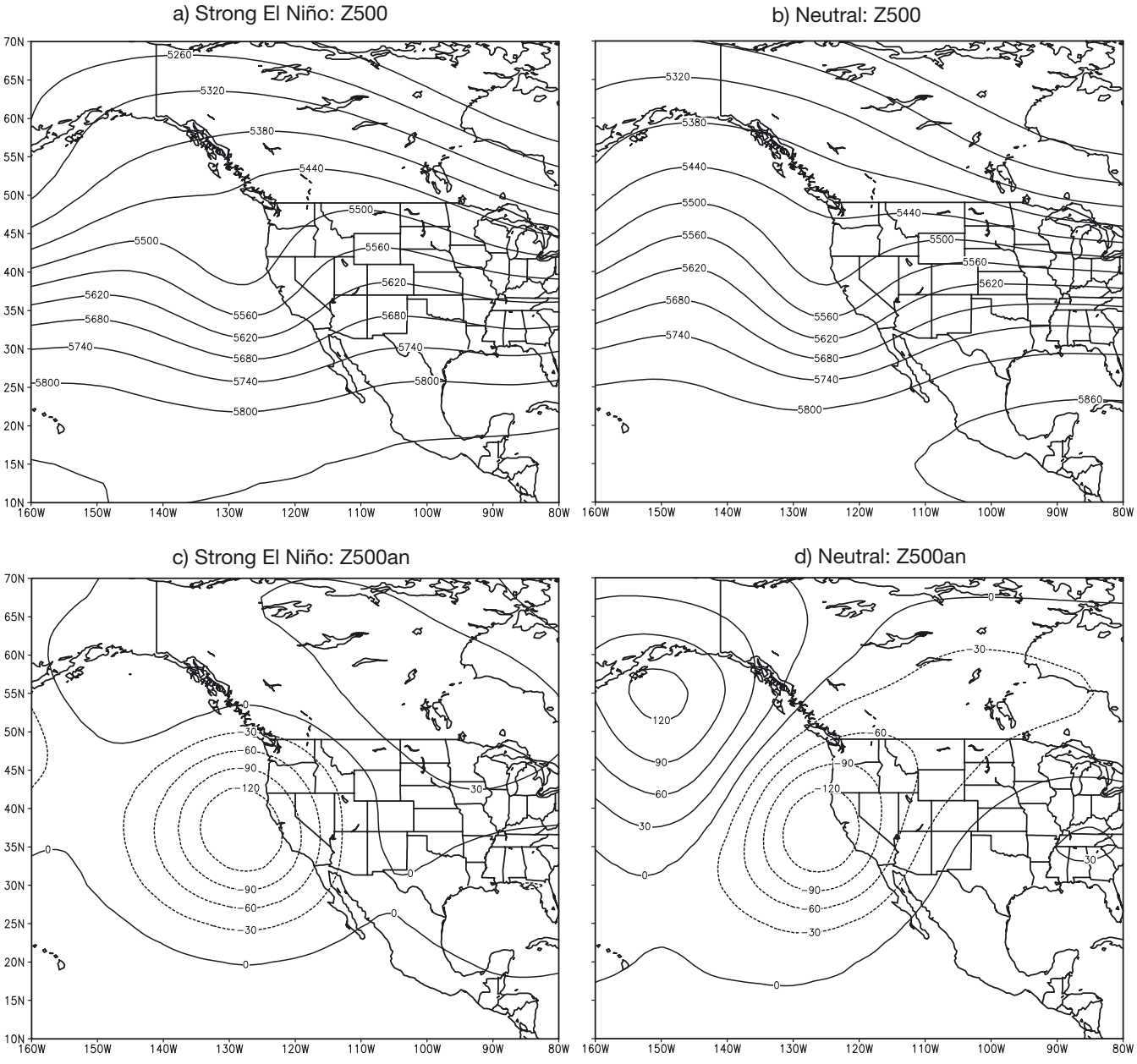

Fig. 6. (a,b) Mean daily composite of 500 hPa geopotential heights (Z500; contour interval = 60 m) characteristic of 1 d extreme precipitation (> 10 mm) events in Tijuana during (a) strong El Niño and (b) neutral years. (c,d) Composite anomalies of Z500 (contour interval = 30 m) for (c) strong El Niño and (d) neutral years. Period: 1976–2000

STR200 anomalies indicate a pronounced negative phase of the tropical/northern hemisphere (TNH) teleconnection pattern (Mo & Livezey 1986), which reflects a southward shift in the storm track associated with the subtropical jet stream. Thus, the TNH significantly modulates the flow of marine air into California, the SW US, and NW Mexico. Pronounced negative phases of the TNH pattern are often observed during winters of strong El Niño events (Barnston et al. 1991).

The Z500 and STR200 composite anomalies of extreme events during neutral years are associated with a southward shift in the negative Pacific/North America (PNA) pattern (Figs 6d & 10b). Horel & Wallace (1981) and Hoerling et al. (1997, 2001) document that most La Niña events are associated with a negative (reverse) PNA pattern, because intense convective activity is found west of the Dateline. However, La Niña events tend to be dry in the study area and are characterized

by the lowest frequency of extreme events (Fig. 4b). This is because the reverse PNA pattern typical of La Niña is usually shifted northwestward (e.g. Hoerling et al. 2001) in Fig. 10b, in such a way that the western trough seen in Figs 6d & 10b would be centered in the Pacific Northwest, where the Pacific jet would produce heavy precipitation. On average, the PNA pattern that produces heavy rainfall over the study area during neu-

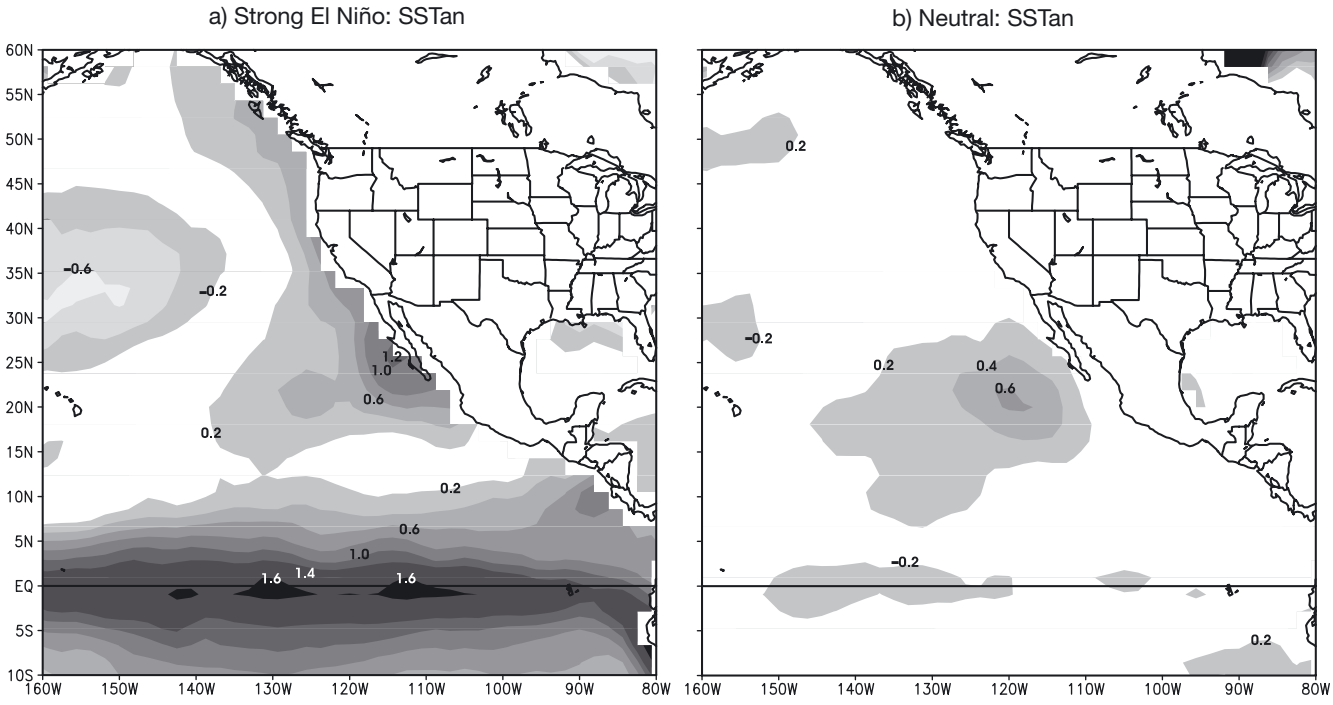

Fig. 7. Mean daily composite anomalies of sea-surface temperature (SST; contour interval = 0.2°C) during 1 d extreme precipitation events of (a) strong El Niño and (b) neutral years. Anomalies are based on the mean period of 1968–1998

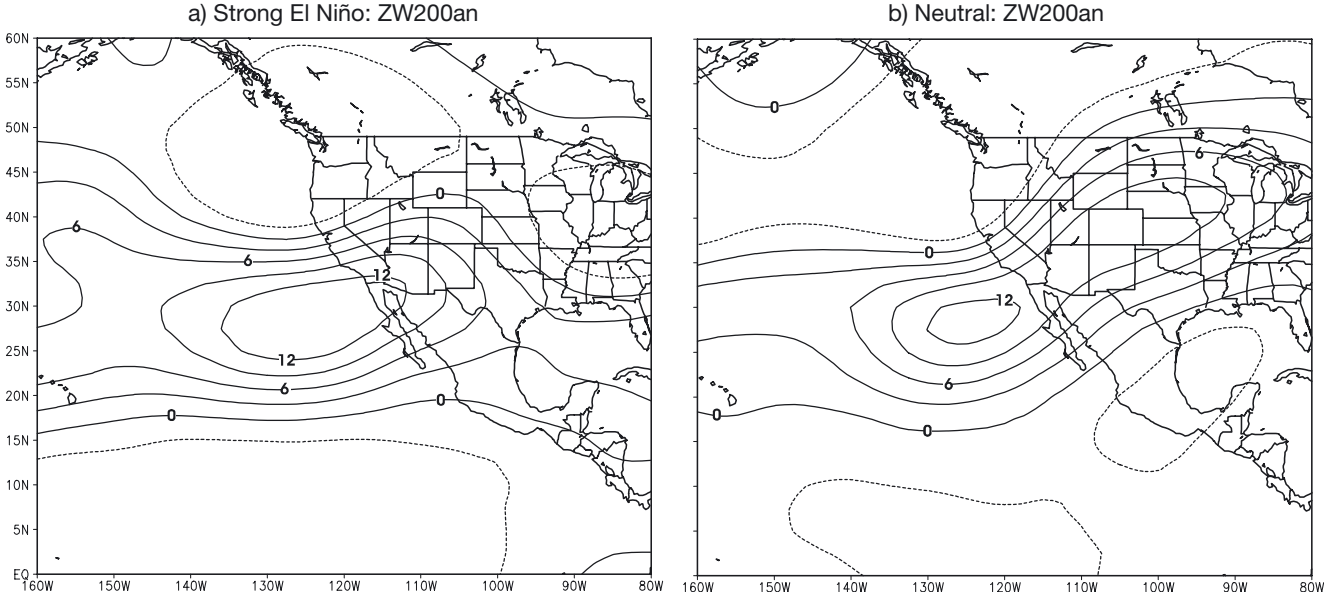

Fig. 8. Mean daily composite anomalies of the 200 hPa zonal wind component (ZW200; contour interval = 3 m s^{-1}) during 1 d extreme precipitation events of (a) strong El Niño and (b) neutral years. Anomalies are based on the mean period of 1968–1998

tral conditions is found between the positive PNA (strong Aleutian low, high over the Rockies/Pacific Northwest and low over Florida: L–H–L) and the reverse PNA (H–L–H); thus, we refer to this variant of the PNA as 'the neutral PNA' (high over the Gulf of Alaska, low over California: H–L). As documented by Hoerling et al. (2001), the wave trains associated with the mid-latitude teleconnections shift westward from El Niño (+PNA, +TNH) to La Niña (–PNA, –TNH).

Tropical heating and associated teleconnections may be the ultimate driver behind the equatorward shift of the jet stream during extreme events. However, diagnostic studies have shown that changes in the storm-track position, through anomalous heat, moisture, and momentum fluxes, often force a larger component of the observed planetary-scale flow anomaly than the imposed external (tropical) forcing (Held et al. 1989, Hoerling & Ting 1994). The southward-displaced jet during extreme conditions (Fig. 8) may provide access to regional low-level moisture from the subtropical Pacific. This is confirmed by the anomalously strong 850 hPa meridional wind component (Fig. 11a,b) that produces low-level moisture advection (i.e. Fig. 11c,d) and instability in the region, possibly affecting the jet through latent heating and positive vorticity advection aloft. The mean January–March low-level moisture (SH850) over southern California and northern Baja California is 3.5 g kg^{-1}; thus the moisture available during extreme events of both strong El Niño and neutral years (Fig. 11c,d) is 50% greater than in normal conditions. This provides a regional thermal forcing to the large-scale disturbance, resulting in strong convective activity and heavy rainfall in southern California and Baja California (Fig. 9).

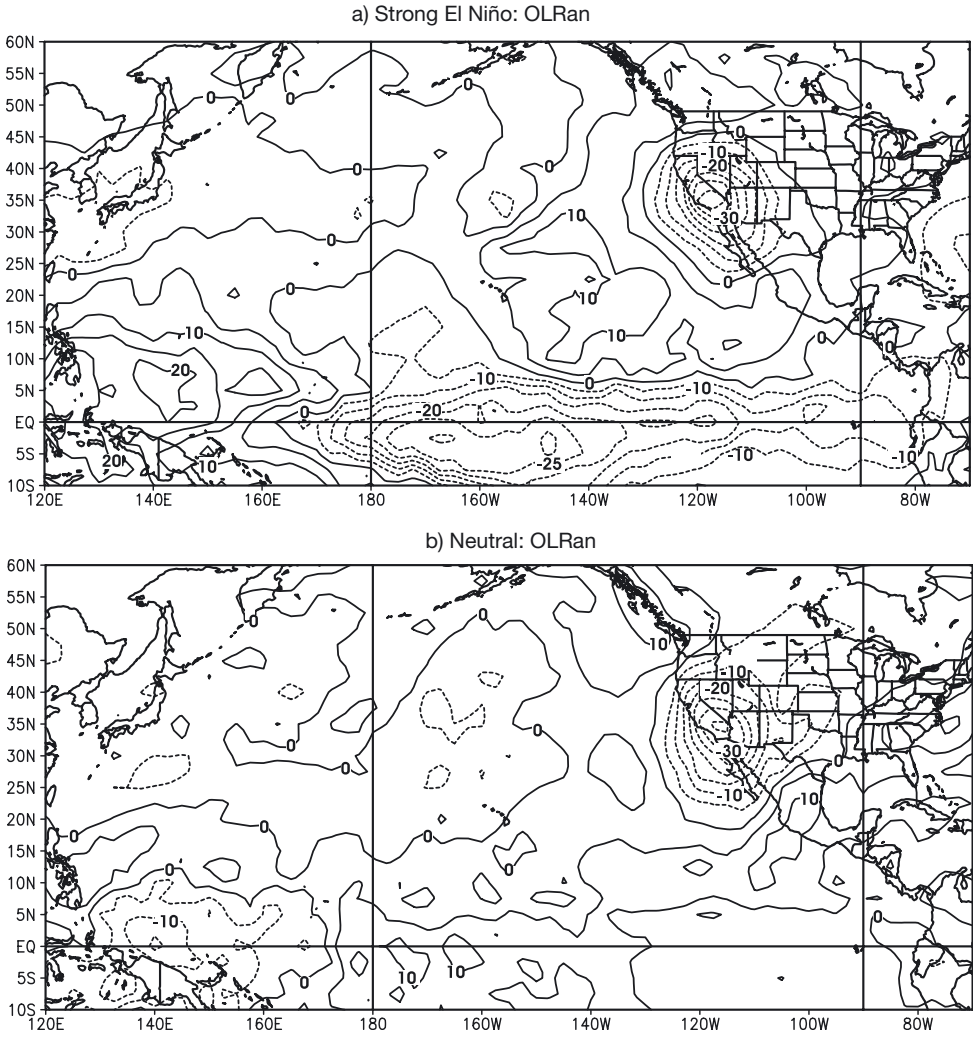

Fig. 9. Mean daily composite anomalies of outgoing longwave radiation (OLR; contour interval = 5 W m^{-2}) during 1 d extreme precipitation events of (a) strong El Niño and (b) neutral years. Anomalies are based on the mean period of 1974–1998

5.2. Evolution of extreme events

In this section we summarize in 2 simple schemes the synoptic evolution (for Days –8,–4 and 0) of the extreme events based on the same diagnostic variables explained in the last section. Fig. 12 shows the evolution of the composite events during strong El Niños only for Days –8 and 0 because the (Rossby) wave train associated with the TNH teleconnection pattern and the enhanced equatorial convection east of the Dateline (160–140° W) were quasi-stationary from Days –12 to +12 of the composite events (as is expected during strong El Niño episodes). An enhanced local Hadley circulation, characterized by intense equatorial convection east of the Dateline dominates the evolution, as exemplified by Day –8 in Fig. 12. The associated upper-level divergence produces a strong and southward-displaced Pacific jet on the convergence zone with maximum westerly zonal winds in the eastern North Pacific (~30° N, 140° W; Fig. 12a); a mid-latitude disturbance (L) on the poleward side of the jet and a tropical moisture surge to the south further intensify the subtropical jet. From Days –8 to 0, the western trough and tropical moisture plume grow, and they slowly move toward the coast of California/Baja California when the jet reaches maximum zonal wind anomalies at the US–Mexico border. At this time, maximum convection and heavy rains are observed over the study area (Fig. 12b). The disturbance reaches Florida by Day +8, but continues to affect the study area at least until Day +4 (not shown).

Fig. 13 shows the schematic evolution of extreme events during neutral conditions. At Day –12, equatorial convection is located west of the Dateline (~160° E,

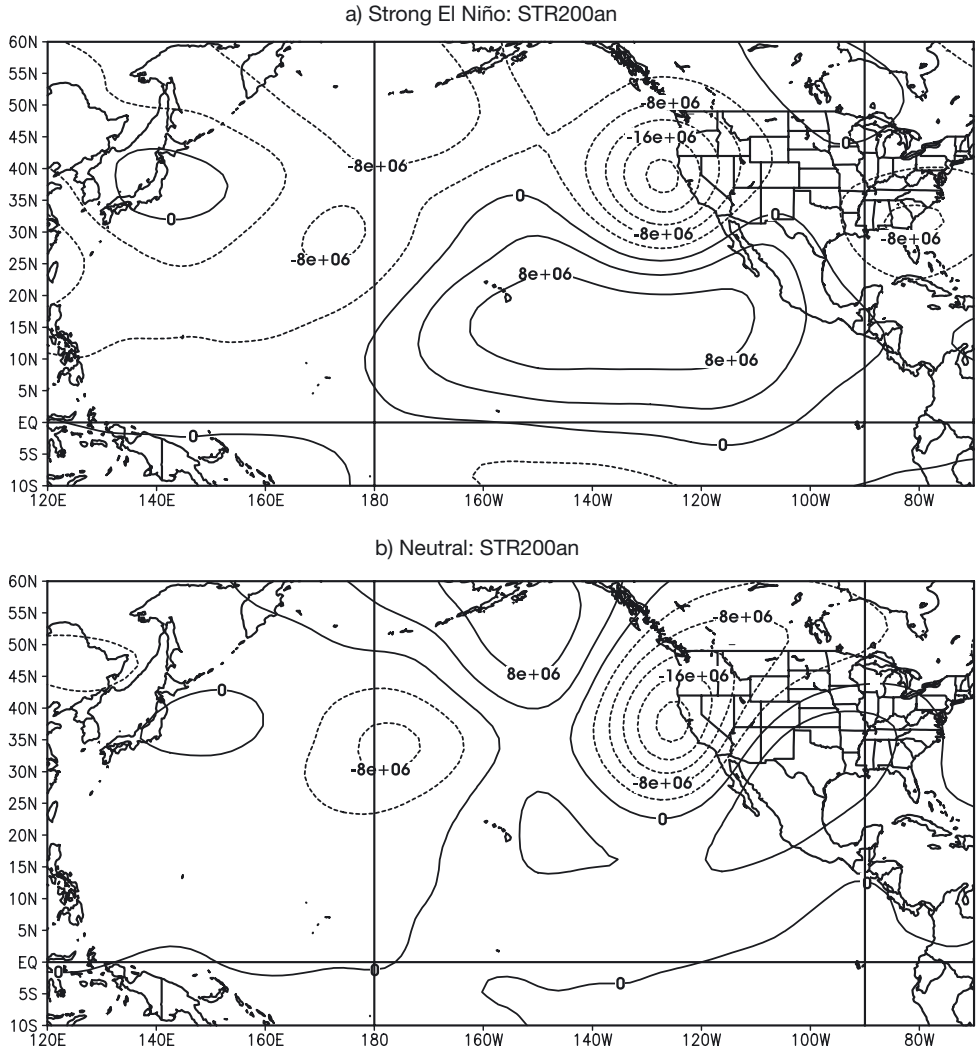

Fig. 10. Mean daily composite anomalies of the 200 hPa streamfunction (STR200; contour interval = 4×10^6 m^2 s^{-1}) during 1 d extreme precipitation events of (a) strong El Niño and (b) neutral years. Anomalies are based on the mean period of 1968–1998

not shown). By Day –8, the equatorial convection migrates to the Dateline, where the jet splits, and a tropical moisture plume extends further NE following the subtropical jet. A blocking high is centered in the Gulf of Alaska, while a weak trough is found near the coast of California. By Day –4, the upper-tropospheric pattern slowly intensifies and retrogrades; convection migrates toward Hawaii, and the moisture plume reaches Baja California. By Day 0, the upper-level circulation pattern continues to retrograde; an intense 'neutral PNA' teleconnection pattern (H–L) is observed in the PNA region, with a deep low over California. At this time, the subtropical jet stream reaches maximum zonal winds along the US–Mexican border, where maximum tropical moisture and convection are also observed, resulting in heavy rains and flooding in southern California and northern Baja California. This type of event is colloquially known as the 'pineapple express' because of the transport of large amounts of moisture from Hawaii, as documented by Higgins et al. (2001) for extreme rainfall events on the US West Coast.

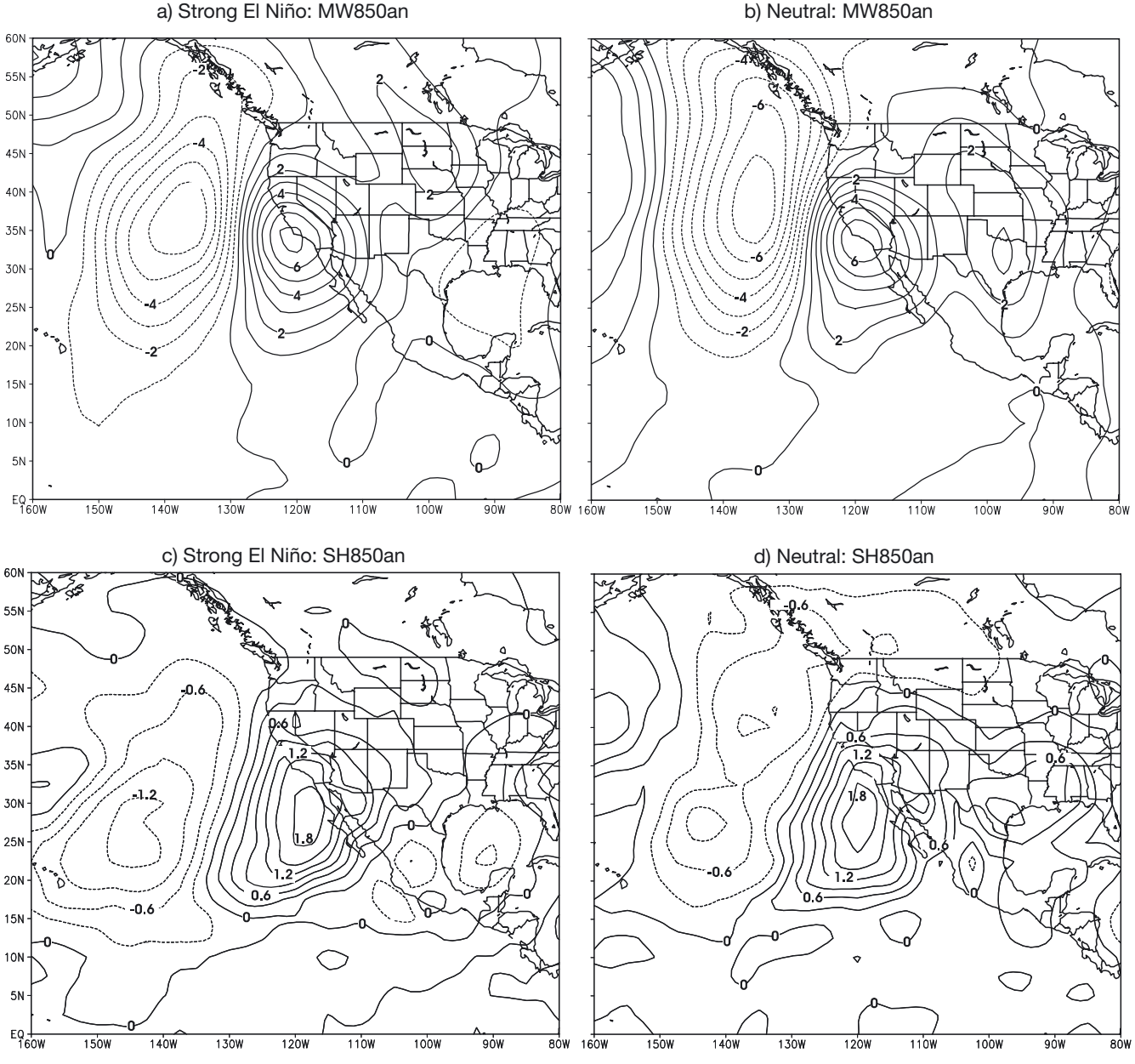

Fig. 11. (a,b) Mean daily composite anomalies of (a, b) the 850 hPa meridional wind component (MW850; contour interval = 1 m s^{-1}); (c,d) 850 hPa specific humidity (SH850; contour interval = 0.3 g kg^{-1}) during 1 d extreme precipitation events of (c) strong El Niño and (d) neutral years

A key factor in the evolution of the 2 types of extreme events analyzed here is the exchange of energy between the tropics and the midlatitudes through the interaction of an anomalous equatorial forcing and a midlatitude disturbance, which are linked by a Rossby wave in the westerlies, leading to an intensified subtropical jet and enhanced storm-track activity in the study area.

6. CONCLUSIONS

Extreme precipitation events in NW Baja California and southern California have produced devastating effects on landscape, natural habitat, personal property, and human life. In particular, extreme events during El Niño have received much media attention in the last 25 yr, not only because of the great extent of their impacts, but also because of the improvement of El Niño's seasonal predictability (e.g. Gershunov & Cayan 2003). In this study on the interannual variability of 1 d precipitation extremes (top 10%) in Tijuana, Baja California, we found that extreme events during neutral (non-ENSO) conditions also play an important role in the extreme climatic variability of the region.

Spectral analysis of winter precipitation indicated that 52% of the variability is linked to the interannual scale (2–7 yr), with ENSO explaining 30% of the rainfall variance. ENSO explains even more (36%) of the variability of 1 d precipitation extremes in the study area. Spectral analysis showed a decadal peak, which explained 23% of the precipitation variance. Mean precipitation and its variability increased after 1976, with a strong impact on the frequency of extreme events in Tijuana. From 1950–1971 to 1976–2000 the total frequency of extreme events increased by almost 100% due to a higher frequency of strong and moderate El Niño episodes as well as to a much stronger influence of neutral conditions on extreme events in the second period. Consistent with our results, Chang & Fu (2003) documented a significant increase in the storm-track activity in the North Pacific over 1979–1999, and Gershunov & Cayan (2003) reported an increase in the frequency of heavy wintertime precipitation events in southern California and the SW US since the late 1970s, apparently in response to the climate 'shift' (Graham 1994) in the North Pacific SST.

We found that extreme events that occur in neutral (strong El Niño) conditions are associated with a 'neutral PNA' (negative TNH) teleconnection pattern that links an anomalous tropical convective forcing west (east) of the Dateline with the southward-displaced Pacific jet over the study area. The neutral PNA is a variant of the typical ±PNA pattern; it is shifted NW of the +PNA (typical of El Niño) and SE of the –PNA (typical of La Niña) and is characterized by a strong ridge over the Gulf of Alaska and a deep low over California.

On average, heavy rainfall during neutral conditions occurred when strong moisture surges from Hawaii, the 'pineapple express', interacted with the subtropical jet and a midlatitude disturbance. Diagnostic studies suggest a nonlinear interaction between tropical heating and the position of the jet through anomalous heat, moisture, and momentum fluxes in the exit region of the jet, which often force

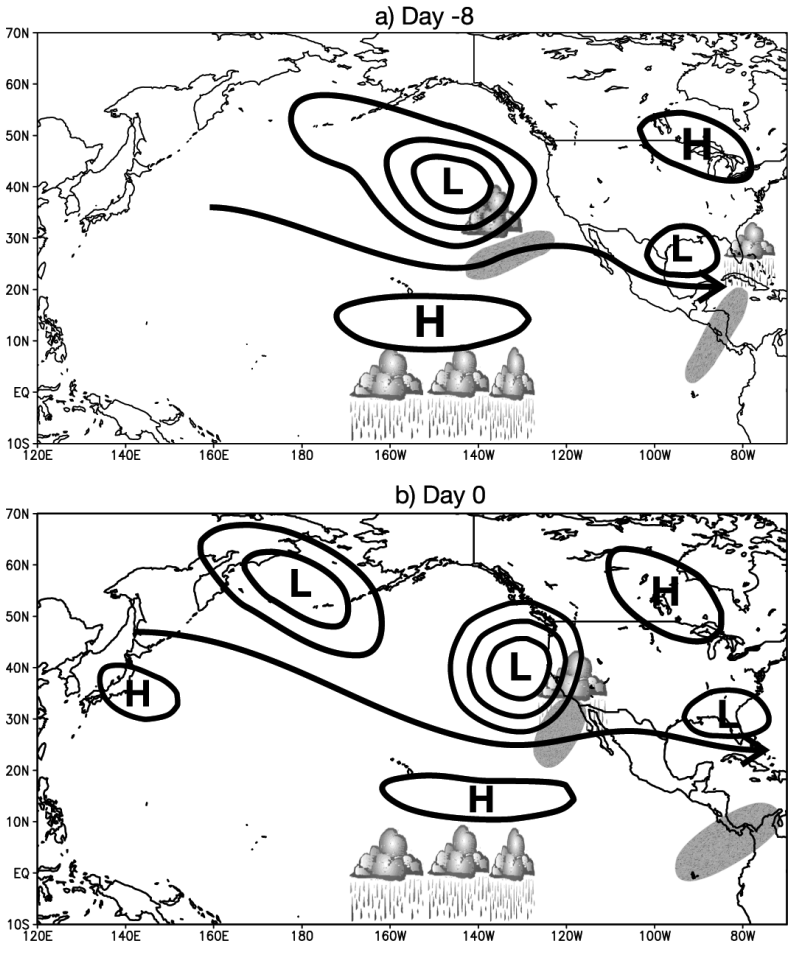

Fig. 12. Schematic evolution of extreme rainfall events in southern California/northern Baja California influenced by strong El Niño conditions for (a) Day –8 and (b) Day 0 (the onset). Clouds represent enhanced convection/precipitation; shaded areas indicate moisture plumes; arrows show the position of the Pacific jet; and highs (H) and lows (L) indicate ridges and troughs based on streamfunction and geopotential height anomalies

a stronger anomaly than the external forcing (Held et al. 1989, Hoerling & Ting 1994). Accordingly, it is possible that the western trough in the jet, typical of extreme events during 1976–2000, was further intensified by thermal interaction with regional anomalies of a warm California Current off Baja California, low-level moisture advection from the subtropical warm sea-surface region, and intense convective activity in the study area. Several authors (Mo & Higgins 1998, Higgins et al. 2000, Jones 2000) have associated the tropical forcing west of the Dateline (i.e. during neutral conditions) to intra-seasonal fluctuations due to the MJO. Our composite evolution of extreme events during neutral conditions also showed a coherent wave train in the North Pacific tied to the equatorial convective anomaly west of the Dateline from Day –12 to the onset of the event. Convection and tropical moisture migrated from west of the Dateline to Hawaii and to the study area in 12 d, while the upper-tropospheric circulation slowly retrograded and intensified in the North Pacific. Thus, it is possible that the well-defined evolution during neutral extreme events is partially modulated by intraseasonal oscillations, which could have some predictability. Furthermore, Gershunov & Cayan (2003) indicated that predictability of heavy precipitation due to neutral influences is lower than that due to ENSO and that it appears to be associated with North Pacific SST interannual and interdecadal variability uncorrelated with ENSO. According to these results, the high variability of extreme events during neutral conditions is due to the interaction of a wide range of scales—from intraseasonal to interdecadal—which explains the difficulty in predicting these extreme conditions. The fact that half of the most catastrophic rainfall events in Tijuana and more than half of the total frequency of 1 d extremes in the 1950–2000 period occurred during neutral conditions shows that it is highly important to gain a better understanding of the forcing mechanisms and predictability associated with non-ENSO conditions.

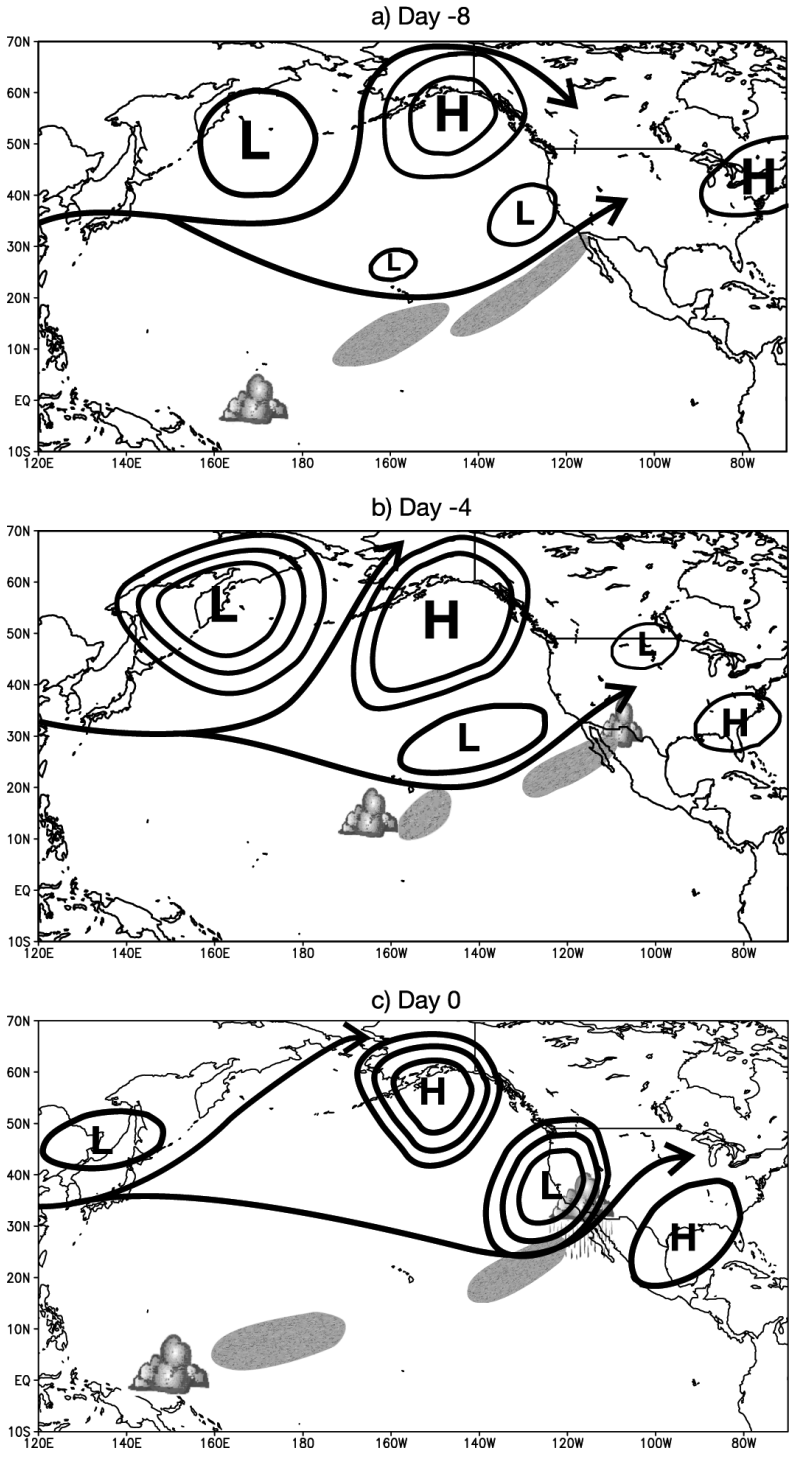

Fig. 13. Schematic evolution of extreme rainfall events in southern California/northern Baja California influenced by neutral conditions for (a) Day –8, (b) Day –4, and (c) Day 0. Details as in Fig. 12

Acknowledgements. This work was supported by NOAA, Office of Global Programs, and the Division of Oceanology, CICESE, Ensenada, Mexico. We are grateful to R. Sanchez of the University of California, Santa Cruz, for his invitation to collaborate in this research. We are thankful to the editor A. Comrie and also to A. Badan, E. Pavía, and 3 anonymous reviewers for their insightful comments and suggestions to earlier versions of this manuscript.

LITERATURE CITED

Aparicio-Mijares FJ (1997) Fundamentos de hidrología de superficie. Limusa, Mexico

AP Worldstream (1998) Flash flood in Mexican border city kills at least 13. Int News 21:57 ET February 8

Barnston AG, Livezey RE, Halpert MS (1991) Modulation of Southern Oscillation–Northern Hemisphere mid-winter climate relationships by the QBO. J Clim 4:203–217

Bjerknes J (1969) Atmospheric teleconnections from the equatorial Pacific. Mon Weather Rev 97:163–172

Bocco G, Sánchez RA, Riemann H (1993) Evaluación del impacto de las inundaciones en Tijuana (Enero de 1993): uso integrado de percepción remota y sistemas de información geográfica. Frontera Norte 5:53–79

Cayan DR, Dettinger MD, Diaz HF, Graham NE (1998) Decadal variability of precipitation over western North America. J Clim 11:3148–3166

Cayan DR, Redmond KT, Riddle LG (1999) ENSO and hydrologic extremes in the western United States. J Clim 12: 2881–2893

Chang EKM, Fu Y (2003) Using mean flow change as a proxy to infer interdecadal storm track variability. J Clim 16: 2178–2196

Chang EKM, Lee S, Swanson KL (2002) Storm track dynamics. J Clim 15:2163–2183

Chatfield C (1975) Time series analysis, theory and practice. Chapman & Hall, London

CNA (Comisión Nacional del Agua) (1995) Programa Estatal Hidráulico, Gerencia Estatal en Baja California, Mexicali

Dedina S (1995) The political ecology of transboundary development: land use, flood control and politics in the Tijuana River Valley. J Borderland Stud X:89–110

Dettinger MD, Cayan DR, Diaz HF, Meko DM (1998) North–south precipitation patterns in western North America on interanual-to-decadal timescales. J Clim 11: 3095–3111

Easterling DR, Evans JL, Groisman PYa, Karl TR, Kunkel KE, Ambenje P (2000) Observed variability and trends in extreme climate events: a brief review. Bull Am Meteorol Soc 81:417–425

Gershunov A, Barnett TP (1998) Interdecadal modulation of ENSO teleconnections. Bull Am Meteorol Soc 79: 2715–2725

Gershunov A, Cayan DR (2003) Heavy daily precipitation frequency over the contiguous United States: sources of climate variability and seasonal predictability. J Clim 16: 2752–2765

Graham NE (1994) Decadal-scale climate variability in the tropical and North Pacific during the 1970s and 1980s—observations and model results. Clim Dyn 10:135–162

Graham NE, Diaz HF (2001) Evidence for intensification of North Pacific winter cyclones since 1948. Bull Am Meteorol Soc 82:1869–1893

Held IM, Lyons W, Nigam S (1989) Transients and the extratropical response to El Niño. J Atmos Sci 46:163–174

Higgins RW (2001) Relationships between temperature extremes, climate variability and long-term trends in the U.S. Clim Rep 2:8–12

Higgins RW, Schemm JK, Shi W, Leetmaa A (2000) Extreme precipitation events in the western United States related to tropical forcing. J Clim 13:793–820

Hoerling MP, Ting M (1994) Organization of extratropical transients during El Niño. J Clim 7:745–766

Hoerling MP, Kumar A, Zhong M (1997) El Niño, La Niña, and the nonlinearity of their teleconnections. J Clim 10: 1769–1786

Hoerling MP, Kumar A, Xu T (2001) Robustness of the nonlinear climate response to ENSO's extreme phases. J Clim 14:1277–1293

Horel JD, Wallace JM (1981) Planetary-scale atmospheric phenomena associated with El Niño-Southern Oscillation. Mon Weather Rev 109:813–829

Jones C (2000) Occurrence of extreme precipitation events in California and relationships with the Madden–Julian Oscillation. J Clim 14:208–218

Karl TR, Easterling DR (1999) Climate extremes: selected review and future research directions. Clim Change 42: 309–325

Karl TR, Knight RW, Plummer N (1995) Trends in high-frequency climate variability in the twentieth century. Nature 377:217–220

Kousky VE, Kayano MT (1994) Principal modes of outgoing longwave radiation and 250-mb circulation for the South Amerian sector. J Clim 7:1131–1143

Liebman B, Smith CA (1996) Description of a complete (interpolated) outgoing longwave radiation dataset. Bull Am Meteorol Soc 77:1275–1277

Lizárraga Arciniega R, Chee-Barragán A, Gil-Silva E, Mendoza-Ponce T, Martínez-Díaz de León A (2003) Effect of El Niño on the subaerial beach Playas de Rosarito, B.C., Mexico. Geofís Int 42:419–428

Madden RA, Julian PR (1972) Description of global-scale circulation cells in the tropics with a 40–50 day period. J Atmos Sci 29:1109–1123

Minnich RA, Viscaino EF, Dezzani RJ (2000) The El Niño/Southern Oscillation and precipitation variability in Baja California, Mexico. Atmosfera 13:1–20

Mo KC, Higgins RW (1998) Tropical convection and precipitation regimes in the western United States. J Clim 11: 2404–2423

Mo KC, Livezey RE (1986) Tropical–extratropical geopotential height teleconnections during the northern hemisphere winter. Mon Weather Rev 114:2488–2515

Pavía EG (2000) Secondary forecast models—the ENSO example. J Appl Meteorol 39:1952–1955

Pavía EG, Badan A (1998) ENSO modulates rainfall in the Mediterranean Californias. Geophys Res Lett 25: 3855–3858

Reyes S, Troncoso R (in press) Multidecadal modulation of winter rainfall in northwestern Baja California. Ciencias Marinas (in press)

Saldaña L (1998) The west coast. In: Water quality in the U.S.–Mexico border region. Borderlines 44:1–10

Schonher T, Nicholson SE (1989) The relationship between California rainfall and ENSO events. J Clim 2:1258–1269

Swetnam TW, Betancourt JL (1998) Mesoscale disturbance and ecological response to decadal climatic variability in the American Southwest. J Clim 11:3128–3147

Trenberth KE, Hurrell JW (1994) Decadal atmosphere–ocean variations in the Pacific. Clim Dyn 9:303–319

Trenberth KE, Branstator GW, Karoly D, Kumar A, Lau N, Ropelewski C (1998) Progress during TOGA in understanding and modeling global teleconnections associated with tropical sea surface temperature. J Geophys Res 103: 14291–14324

Zhang Y, Held IM (1999) A linear stochastic model of a GCM's midlatitude storm tracks. J Atmos Sci 56:3416–3435

Zhang Y, Wallace JM, Battisti DS (1997) ENSO-like interdecadal variability: 1900–93. J Clim 10:1004–1020

Editorial responsibility: Andrew Comrie, Tucson, Arizona, USA

Submitted: October 18, 2002; Accepted: November 14, 2003
Proofs received from author(s): January 15, 2004